

CHEOPS's hunt for exocomets: photometric observations of 5 Vul Rebollido, I.; Zieba, S.; Iglesias, D.; Bourrier, V.; Kiefer, F.; Lecavelier Des Etangs, A.

Citation

Rebollido, I., Zieba, S., Iglesias, D., Bourrier, V., Kiefer, F., & Lecavelier Des Etangs, A. (2023). CHEOPS's hunt for exocomets: photometric observations of 5 Vul. *Monthly Notices Of The Royal Astronomical Society*, *523*(1), 1441-1447. doi:10.1093/mnras/stad1475

Version: Publisher's Version

License: <u>Creative Commons CC BY 4.0 license</u>
Downloaded from: <u>https://hdl.handle.net/1887/3719344</u>

Note: To cite this publication please use the final published version (if applicable).

Downloaded from https://academic.oup.com/mnras/article/523/1/1441/7165768 by Universiteit Leiden - LUMC user on 21 February 2024

CHEOPS's hunt for exocomets: photometric observations of 5 Vul

Isabel Rebollido [®], ¹★ Sebastian Zieba, ^{2,3} Daniela Iglesias [®], ⁴ Vincent Bourrier, ⁵ Flavien Kiefer and Alain Lecavelier Des Etangs ⁶

Accepted 2023 May 10. Received 2023 May 10; in original form 2022 October 26

ABSTRACT

The presence of minor bodies in exoplanetary systems is in most cases inferred through infrared excesses, with the exception of exocomets. Even if over 35 yr have passed since the first detection of exocomets around β Pic, only \sim 25 systems are known to show evidence of evaporating bodies, and most of them have only been observed in spectroscopy. With the appearance of new high-precision photometric missions designed to search for exoplanets, such as *CHEOPS*, a new opportunity to detect exocomets is available. Combining data from *CHEOPS* and *TESS* we investigate the light-curve of 5 Vul, an A-type star with detected variability in spectroscopy, to search for non-periodic transits that could indicate the presence of dusty cometary tails in the system. While we did not find any evidence of minor bodies, the high precision of the data, along with the combination with previous spectroscopic results and models, allows for an estimation of the sizes and spatial distribution of the exocomets.

Key words: comets: general – stars: individual: HD182919.

1 INTRODUCTION

Exocomets are still the only minor bodies we are able to observe in extrasolar planetary systems. However, they remain elusive, and since their first detection by Ferlet, Hobbs & Vidal-Madjar (1987) around the star β Pictoris, only other \sim 25 systems show evidence of the presence of such minor bodies (Strøm et al. 2020). The first evidences for exocomets were observed in spectroscopy, as (blue-)red-shifted variations in the Ca II K lines of several A-type stars, with a sample growing slowly throughout the years (e.g. Redfield & Linsky 2008; Montgomery & Welsh 2012; Kiefer et al. 2014b; Rebollido et al. 2020). The variations observed spanned from few to hundreds of kilometres per second, and traced the gaseous tails of exocomets as they transited the star. They were found later in ultraviolet wavelengths, tracing other metallic elements (Vidal-Madjar et al. 1994; Roberge et al. 2000; Grady et al. 2018). Due to the sporadic nature of exocometary events, their orbits are difficult to constrain, and only for the case of β Pic we have estimations of the pericentre of the transiting comets, both through models (Beust & Morbidelli 1996, 2000) and observations (Kennedy 2018).

Given comets in the Solar system develop two tails, one composed of gas and another one composed of dust, it was predicted (Lecavelier Des Etangs 1999; Lecavelier Des Etangs, Vidal-Madjar & Ferlet 1999) that photometric observations could also detect these bodies as individual (i.e. non-periodic) transits, with a particular saw tooth shape due to the exponential decrease of material in the tail. While

observations compatible with exocomets were detected with *Kepler* (Boyajian et al. 2016; Rappaport et al. 2018; Kennedy et al. 2019), the sensitivity and pointing constrains of the instrument did not allow for observations of the bright A-type stars where exocomets have been classically found using spectroscopy. Shortly after, the launch of *TESS* allowed monitoring of much brighter stars, leading to the detection of exocomets in photometry in the star β Pic (Zieba et al. 2019; Pavlenko et al. 2022) with a frequency high enough to make estimations about the size distribution of the minor bodies in the system (Lecavelier des Etangs et al. 2022). To this date, there are no publication of simultaneously detected comets in spectroscopy and photometry around any star.

Aiming at expanding the sample of known spectroscopic exocomet host stars with photometric detections, we obtained *CHEOPS* Cycle 1 data of the star 5 Vulpecula, selected as at the time of the call for proposals it did not fall in the *TESS* observing windows. The structure of the paper is as follows: Section 2 describes the target and observations; Section 3 analyses the photometric upper limits and revises the published spectroscopic data; Section 4 offers an overview of the system and the potential discrepancy between observation strategies; and finally Section 5 summarizes the work presented here.

2 TARGET AND OBSERVATIONS

2.1 5 Vul

5 Vul (HD 182919) is an A-type star with a detected debris disc (*Spitzer* mid-infrared (IR) data; Morales et al. 2009). The most relevant data are summarized in Table 1. Chen et al. (2014) reported

¹Space Telescope Science Institute, Baltimore, MD 21218, USA

²Max-Planck-Institut für Astronomie, Königstuhl 17, D-69117 Heidelberg, Germany

³Leiden Observatory, Leiden University, Niels Bohrweg 2, NL-2333CA Leiden, the Netherlands

⁴School of Physics and Astronomy, Sir William Henry Bragg Building, University of Leeds, Leeds LS2 9JT, UK

⁵Observatoire Astronomique de l' Universitè de Genève, Chemin Pegasi 51b, CH-1290 Versoix, Switzerland

⁶Institut d' Astrophysique de Paris, Sorbonne Universitè, 98bis Boulevard Arago, Paris, 75014, France

^{*} E-mail: irebollido@cab.inta-csic.es

1442 I. Rebollido et al.

Table 1. Stellar parameters for 5 Vul.

Name	RA (2000)	DEC (2000)	SpT	$v_{\rm rad}$ (km s ⁻¹)	$T_{\rm eff}$ (K)	logg (cgs)	$v\sin{(i)} (km s^{-1})$	Distance (pc)	V (mag)	Age Myr
5 Vul	19:26:13.25	+20:05:51.8	A0V	-24.3 ± 1.4	10460 ± 80	4.47 ± 0.10	154	71.98	5.59	198

Note. Distance and coordinates were obtained from *Gaia* (Gaia Collaboration 2016, 2018), age from Chen et al. (2014), and v_{rad} , T_{eff} , log g, and $v_{\text{sin}i}$ from Rebollido et al. (2020). V is from Simbad.

a $L_*/L_{\rm IR}$ of 3.3 x 10⁻⁵, and the presence of a double belt with temperatures of 295 and 100 K for the inner and outer belts, respectively. The first evidence of a gaseous environment around 5 Vul was reported in Montgomery & Welsh (2012), where a Falling Evaporating Bodies (FEB)-like event was observed at ~50 km s⁻¹, and further variations were also reported by Rebollido et al. (2020).

We selected 5 Vul as an optimal target for *CHEOPS* observations among other exocomet-host stars due to its proximity (less than 100 pc) and brightness ($V \sim 5.6$). At the time when the call for proposals for *CHEOPS* Cycle 1 closed, 5 Vul was not expected to be observed by the primary mission of *TESS* as it fell in the CCD gap, unlike other exocomet-host stars. It was also not observed by K2 due to its height relative to the ecliptic and brightness (V = 5.59). Posterior changes in *TESS* schedule permitted observations of the target, which are also included in this work.

2.2 Observations and data reduction

2.2.1 CHEOPS

The CHEOPS (Benz et al. 2021) data were taken as part of program CH_PR210021 ('Hunting for exocomets transiting the young nakedeye star 5 Vulpeculae'; PI Rebollido) between 2020 June 29 and 2020 July 1 (see Table 2). Due to the objective of observing a nonperiodic transit, the observations were targeted to be non-interrupted, and led to one visit over a duration of 44.96 h. Data were processed with the latest version of the CHEOPS automatic data reduction pipeline (DRP; v13.1.0). The pipeline corrects the raw images (bias subtraction, gain conversion, flat-fielding, dark correction, and nonlinearity) and then performs aperture photometry. An example for a CHEOPS exposure can be found in Fig. 1. A detailed description of DRP can be found in Hoyer et al. (2020). The pipeline outputs lightcurves with differently sized apertures: R = 25.0 pixels (DEFAULT), R = 22.5 pixels (RINF), R = 30.0 pixels (RSUP), and R = 26.5(OPTIMAL). The latter maximizes the signal-to-noise ratio (SNR) of the photometry by maximizing the flux coming from the target while minimizing the flux from background stars. This SNR calculation, performed by the DRP, uses the Gaia catalogue and the point spread function (PSF) shape of CHEOPS. The OPTIMAL aperture has a resulting point-to-point root-mean-square (rms) of 63.9 ppm, which is the lowest of all considered apertures. We therefore chose the OPTIMAL aperture for our analysis. Fig. 2, top panel, shows the CHEOPS light-curve used in this analysis. Flagged observations (which might indicate cosmic ray events or crossing of the South Atlantic Anomaly) and outliers greater than 4σ with respect to the median have been removed. These make up approximately 4 per cent of the total observations. The corresponding periodogram is shown in the bottom panel of Fig. 2. The vertical dashed lines indicate the multiples of 14.5 cpd (\sim 100 min), corresponding to the orbital breaks of the satellite. No other frequencies show significant peaks.

2.2.2 TESS

5 Vul (TIC 359600295) was observed by *TESS* (Ricker et al. 2015) in Sector 14 from 2019 July 18 to 2019 August 14, in Sector 40

from 2021 June 25 to 2021 July 23, and in Sector 54 from 2022 July 9 to 2022 August 4 at a 2 min cadence (see Table 2). Data were processed by the TESS Science Processing Operations Center (SPOC) pipeline (Jenkins et al. 2016) and accessed using the Python package lightkurve (Lightkurve Collaboration et al. 2018) which downloads the data from the Mikulski Archive for Space Telescopes archive.1 Target pixel files (TPFs) are shown in Fig. 3. For this analysis, we used the pre-search data conditioning simple aperture photometry (PDCSAP, Smith et al. 2012; Stumpe et al. 2012, 2014) light-curves. In contrast to the simple aperture photometry lightcurves, the PDCSAP data are corrected for instrumental systematic effects and show considerably less scatter and variability caused by instrumental events like momentum dumps. The PDCSAP lightcurves were flagged by the SPOC pipeline for bad data which mark anomalies like instrumental issues or cosmic ray events. We removed any TESS exposure in our data set with a non-zero 'quality' flag. For Sector 14, scattered light from the Earth was saturating the part of the detector where 5 Vul hit on silicon.² We excluded these times which occurred in the last quarter of each orbit (see Fig. 4 around BTJD 1691–1694 and BTJD 1705–1708). The breaks of approximately 1 d in the middle of each Sector, are related to the data downlink of TESS when it reaches its perigee. Fig. 4 shows that any significant changes in flux occur at the beginning or at the end of an TESS orbit or during momentum dumps and are therefore not caused by the star itself. In total, we removed approximately 7 per cent of the TESS data mostly due to saturation of Camera 1 in Sector 14. Fig. 3 shows the pointing of TESS in Sector 14, 40, and 54, showing that there are no close, bright stars nearby which could bias our flux measurements.

The *TESS* data do not show any significant periodic signals which could be attributed to stellar variability (see Fig. 5). Systematic signals at very short periods, such as the orbit of *TESS* around Earth, with a period of 14 d can be hinted from Fig. 4.

3 ANALYSIS OF RESULTS

There is no detection of flux fluctuations indicative of the presence of exocometary activity in the light-curve of 5 Vul or any other transits with a significative depth ($>5\sigma$) after the analysis reported in Section 2.2. However, we can estimate comet sizes for a given trajectory based on the upper limits.

3.1 Detectability

Exocomets have been previously detected with *Kepler* (formally *K2*, Boyajian et al. 2016; Rappaport et al. 2018) and *TESS* (Zieba et al. 2019). While those missions were not designed for this particular science case, both have provided interesting results. The first detection of exocomets around a star with a spectral type different

¹https://archive.stsci.edu/missions-and-data/tess

²For more information, see the Data Release Note of Sector 14 at: https://archive.stsci.edu/missions/tess/doc/tess_drn/tess_sector_14_drn19_v02.pdf ³BTJD (Barycentric TESS Julian Date) = BJD—2457000.0 d.

Table 2. Observations with TESS and CHEOPS used in this work.

Observation	Start date (UTC)	End date (UTC)	Exp. time (s)
TESSS14	2019-Jul-18 20:35:54	2019-Aug-14 16:59:19	120
TESSS40	2021-Jun-25 03:46:55	2021-Jul-23 08:35:25	120
TESSS54	2022-Jul-09 09:41:08	2022-Aug-04 15:11:01	120
CHEOPS	2020-Jun-29 13:16:11	2020-Jul-01 10:13:44	44

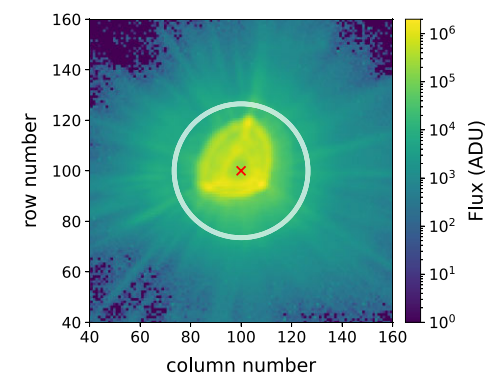


Figure 1. A *CHEOPS* exposure showing the typical PSF shape of the instrument, including the centroid of the star as determined by the DRP marked with a red cross and the OPTIMAL aperture being shown with a white circle.

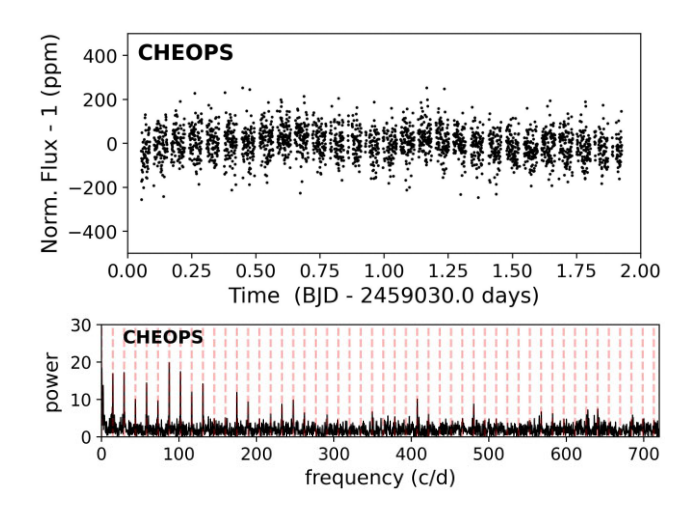


Figure 2. Top panel: Full *CHEOPS* light-curve. Normalized and outliers removed. Bottom panel: Periodogram corresponding to *CHEOPS* data. Vertical red dashed lines show peaks at multiples of 14.5 cpd (\sim 100 min), corresponding to the orbital breaks of the satellite.

than A was in photometry, using K2 data (Rappaport et al. 2018), and the detection of photometric exocomets around β Pic, the only star with exocomet detection using two different techniques, used TESS data (Zieba et al. 2019).

When compared to those missions, *CHEOPS* provides very similar capabilities. The cadence of *CHEOPS* observations is shorter (1 min), but comparable to *TESS* and *Kepler* (2 min). The photometric precision, however, is much better, with an estimated 10 ppm for a V=6 star against ~ 50 ppm for *TESS* (Ricker et al. 2015) and while a number of bright targets were observed with *Kepler* (e.g. Guzik et al. 2016), the magnitude of 5 Vul exceeded *Kepler*'s nominal mission, and it was never observed. The response of the detectors is very unlikely to be responsible for detection rates

either, since it is very similar to *TESS* and practically identical to *Kepler*.⁴

Therefore, the non-detection in this target is most likely related to the lack of exocometary transits at the time of observations, as explained in Section 4.2, and not to the instrumental capabilities.

3.2 Maximum exocomet size

Given that there is previous evidence of exocomets in the system, we explore the range of sizes and periastrons that we are sensitive to. We propose two different approaches for the size estimation, and test them for the different detection limits of both observatories.

3.2.1 Estimation based on Hill spheres

Assuming exocomets have very eccentric orbits (Beust & Morbidelli 2000), the more volatile materials evaporate as they come closer to the central star, developing a coma composed by the evaporating gas and the dust dragged by it. If we consider all the material in the coma to be optically thick and gravitationally bound to the nucleus, we can follow Boyajian et al. (2016) approximation, and estimate the maximum exocomet nucleus size we would be able to detect given the SNR of our light-curve.

The depth of the transit, τ , is directly related to the surface of the star covered by the comet, and for two spherical bodies can be expressed as a function of the ratio of their radius, r and R_* for the comet and star, respectively:

$$\tau = \left(\frac{r}{R_*}\right)^2.$$

Given our SNR, we would not be able to detect transits smaller than 5.85×10^{-3} per cent (58 ppm) for *TESS* and 1.38×10^{-3} per cent (13 ppm) for *CHEOPS* (see Figs 2 and 4).

To retrieve the size of the comet associated to the clump, we can take into account the definition of Hill radius as:

$$R_{\rm Hill} = a(1-e) \left(\frac{M_{\rm comet}}{3M_*}\right)^{1/3}.$$

Given we are estimating all our material is optically thick, we can assume $\tau \sim R_{\rm Hill}$. The minimum periastron values are limited by our cadence (1 min for *CHEOPS* and 2 min for *TESS*) following *Kepler's* third law, and are consistent with the estimations for exocometary orbits for β Pic (Lecavelier des Etangs et al. 2022). The obtained mass for the cometary nucleus can then be converted to radius considering a typical density for a comet of 0.5 g cm⁻³ (Britt, Consolmagno & Merline 2006).

Fig. 6 shows in red the minimum size of the exocometary nucleus for an A0V star (2.193 R_{\odot} and 2.18 M_{\odot} ; Pecaut & Mamajek 2013).

⁴More information about the *CHEOPS* bandpass and its comparison with previous missions can be found at: https://www.cosmos.esa.int/web/cheops/performances-bandpass

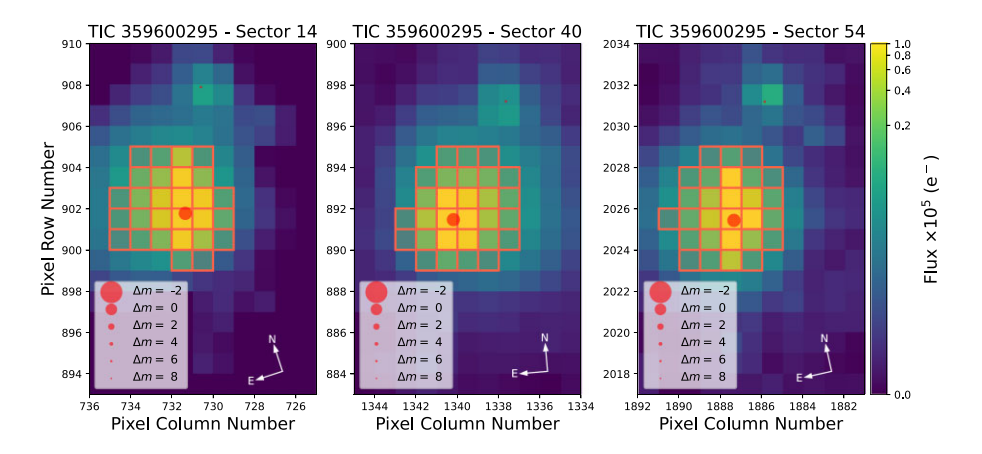


Figure 3. TESS TPFs for 5 Vul in Sector 14, 40, and 54. The pixels shaded in red indicate the aperture used by the SPOC pipeline. There are no stars within the aperture of 5 Vul with a *Gaia* magnitude difference smaller than 8, meaning background stars do not significantly contribute to the measured flux of 5 Vul. Plot is made using tpfplotter (Aller et al. 2020).

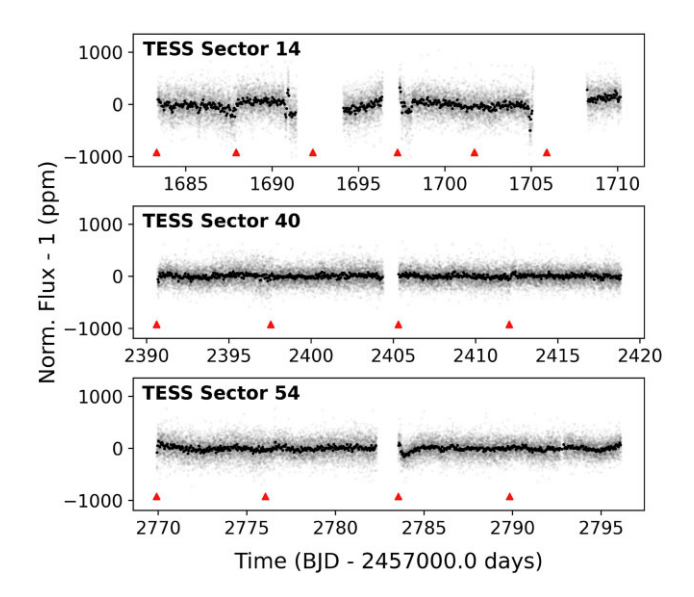


Figure 4. Full *TESS* light-curve. Telescope momentum dumps are marked with red arrows. The 2 min cadence *TESS* data (shown in light grey) have been binned to time-scales of an hour for better visualization.

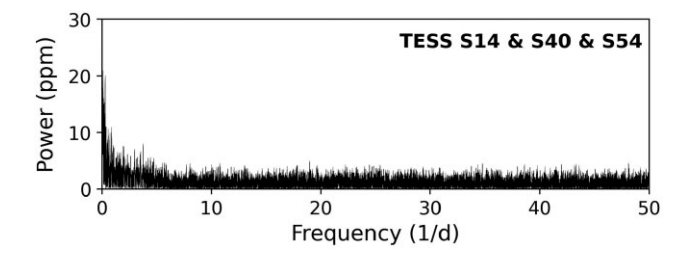


Figure 5. Lomb–Scargle periodogram of the full TESS light-curve.

From this calculation, we can estimate that anybody that transited the star during the observations must have had a nucleus smaller than ~ 5.2 km for *CHEOPS* and ~ 10.7 km for *TESS* at a distance of 1 au. The fact that the increase in distance allows to trace smaller bodies is based on our first assumption of all material released in the evaporation process is contained in the Hill sphere and optically thick, which might not be a realistic approximation. Actually, assuming a similar composition throughout the system, the further from the star

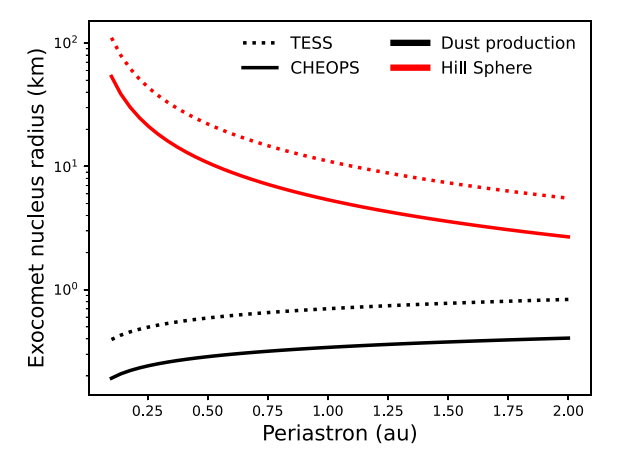


Figure 6. Minimum exocomet nucleus size estimates accessible with both *CHEOPS* (solid line) and *TESS* (dotted line) observations as a function of periastron distance. Red lines show size estimations for a spherical exocometary body with all the opaque material gravitationally bound to the central body (Hill sphere). Black lines show size estimations based on dust production rates.

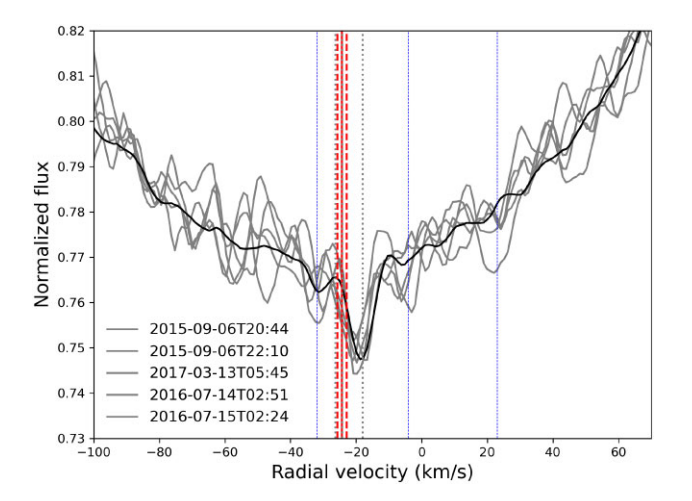


Figure 7. Spectroscopic evidence of exocomets in 5 Vul. Variations are seen at -3.5, 23, and $-31 \,\mathrm{km}\,\mathrm{s}^{-1}$, indicated by the blue vertical lines. Red vertical lines show the radial velocity of the object $(-24.3 \pm 1.4 \,\mathrm{km}\,\mathrm{s}^{-1})$, and grey vertical lines show the radial velocity of the ISM in the line of sight $(-18.05, -24.21, \mathrm{and} -26.30 \,\mathrm{km}\,\mathrm{s}^{-1})$.

the exocomet is, the less material we are able to extract from the comet due to the inverse squared dependence of stellar flux with distance. Therefore, in the next section we explore a size estimation that contains evaporation models.

3.2.2 Estimations based on dust production rates

Following the calculation made by Lecavelier des Etangs et al. (2022), we can estimate the corresponding minimum exocomet dust production rate that we would be able to detect with our light-curves.

The typical absorption depth (AD) in a light-curve that is caused by the transit of an exocomet is given by Lecavelier des Etangs et al. (2022):

$$\mathrm{AD} = 5 \cdot 10^{-5} \left(\frac{\dot{M_{1\mathrm{au}}}}{10^5 \, \mathrm{kg/s}} \right) \left(\frac{q}{1 \, \mathrm{au}} \right)^{-1/2} \left(\frac{M_{\star}}{\mathrm{M}_{\odot}} \right),$$

where \dot{M}_{1au} is the comet dust production rate taken at 1 au from the star, q is the comet orbit periastron distance, and M_{\star} the mass of the star. Therefore a detection limit in AD can be translated into a corresponding maximum dust production rate. For a stellar mass $M_{\star} = 2.18 \text{ M}_{\odot}$ (Pecaut & Mamajek 2013), we obtain

$$\dot{M_{1au}} = 1.2 \times 10^4 \,\mathrm{kg} \,\mathrm{s}^{-1} \left(\frac{\mathrm{AD}}{13 \,\mathrm{ppm}}\right) \left(\frac{q}{1 \,\mathrm{au}}\right)^{1/2}.$$

Recalling that the Hale-Bopp comet had a dust production rate in the order of $2 \times 10^6 \text{ kg s}^{-1}$ at 1 au from the Sun, we see that the *CHEOPS* observations are very sensitive to small comets.

Similarly as done by Lecavelier des Etangs et al. (2022), the dust production rate can be converted into a corresponding radius of the cometary nucleus using the relationship:

$$\dot{M}_{1au} = 2 \cdot 10^6 \,\mathrm{kg/s} \left(\frac{R}{30 \,\mathrm{km}}\right)^2 \left(\frac{L_{\star}}{\mathrm{L}_{\odot}}\right),$$

where R is the radius of the comet nucleus and L_{\star} the stellar luminosity, and we are considering a typical cometary radius and dust production similar to Hale-Bopp (Fernández et al. 1999; Jewitt & Matthews 1999). With a luminosity of about 40 L_{\odot} for the A0 star 5 Vul (Yoon et al. 2010), we finally have

$$R = 0.36 \,\mathrm{km} \left(\frac{\mathrm{AD}}{\mathrm{13 \, ppm}}\right)^{1/2} \left(\frac{q}{\mathrm{1 \, au}}\right)^{1/4}.$$

When taking into account the evaporation models, it appears that the presented *CHEOPS* and *TESS* observations with no exocomet photometric transit detection allow us to exclude the transit of very small bodies (0.3 km for *CHEOPS* and 0.7 km for *TESS*) at 1 au over the observation period.

4 DISCUSSION

The detection of exocomets using photometric data has been restricted to a few systems so far. Contrary to what is observed in spectroscopy, where most comets are found around A-type stars (e.g. Rappaport et al. 2018; Kennedy et al. 2019), the detections in photometry do not seem to be restricted to a certain spectral type. In the following, we discuss the properties of 5 Vulpeculae, and what might be the origin of the discrepancy of the spectroscopic and photometric data.

4.1 Disc and planets

A faint debris disc is located in the environment of 5 Vul. Chen et al. (2014) report significant excess for wavelengths longer than

24 µm corresponding to a faint and likely not very massive disc, especially when compared to other debris discs around A-type stars. They fit two components to the disc, with two different blackbody (BB) temperatures, being the most massive the colder component (10⁻⁵ M_⊕), at a distance of 34 au and with a BB temperature of ~100 K. More recently, Musso Barcucci et al. (2021) reported a detection of the disc in band L, and fitted a single BB at \sim 23 au, with a temperature of \sim 180 K. The main goal of that paper was to look for planetary companions, and they also report 5σ mass limits for all the investigated stars, including 5 Vul. However, the precision achieved can only estimate an upper limit for our system of $> 20 \,\mathrm{M_{I}}$ at distances shorter than 50 au, twice the mass of β Pic b. Their analysis of the self-stirring mechanisms (see fig. A4 in Musso Barcucci et al. 2021) indicate that the disc is not large enough to produce the observed dust, and possibly a perturber (planet, companion, and binary star) is affecting the system dynamics. Matthews et al. (2018) also reported no planetary companions larger than 8 M_J at distances larger than 10 au based on SPHERE observations in H2 and H3. Despite having hot Ca II gas detected, located very close to the star (see Fig. 8) and a known debris disc, there is no detection of cold gas in the outer regions of the system (see e.g. Marino et al. 2020, and references therein for an overview of CO gas around A-type stars). Rebollido et al. (2022) report an upper mass limit for the dust and CO content based on ALMA observations of $\sim 10^{-3}$ and 10^{-6} M_{\oplus}, respectively, consistent with previous models (Kral et al. 2017). The age of 5 Vul, estimated around 200 Myr (Chen et al. 2014) could potentially explain the low fractional luminosity and the lack of CO gas due to a decrease in dynamical activity as the system settles.

4.2 Spectroscopic counterpart in 5 Vul

The investigation of the 5 Vul spectra has revealed the presence of exocomets, reported in Montgomery & Welsh (2012) and Rebollido et al. (2020). We show in Fig. 7 spectra previously published in Rebollido et al. (2020) and publicly available online. The exocometary events were detected within -5 and $60~{\rm km\,s^{-1}}$ in both cases, with one extra tentative detection located at $-35~{\rm km\,s^{-1}}$. The poor time coverage does not allow for a follow-up of the events. Moreover, both papers report variability of the more stable component (at $\sim\!-20~{\rm km\,s^{-1}}$ consistent with the radial velocity of the star, but also with the G interstellar cloud; Redfield & Linsky 2008), suggesting at least a partially circumstellar origin and variations in the amount of circumstellar gas.

There are 39 spectra in Rebollido et al. (2020) spanning 22 nights, which overall show variable absorptions both blue- and red-shifted in approximately 20 per cent of the observations. This is consistent with a frequency of one detected variation every 4.2 d. Montgomery & Welsh (2012) show one exocometary red-shifted absorption in four spectra, and small variations in the EW measurements of the stable feature that seem gradual with time (see fig. 3 and table 2 of Montgomery & Welsh 2012), again consistent with variations in 20 per cent of the observations.

4.3 Photometric comets versus spectroscopic comets

The only star where exocomets have been found both in spectroscopy and photometry is β Pic (Ferlet et al. 1987; Kiefer et al. 2014a; Zieba et al. 2019). The high frequency observed in spectroscopy, of around one exocometary absorption observed every hour to 6 h, surpasses

⁵ESO archive and https://doi.org/10.26093/cds/vizier.36390011.

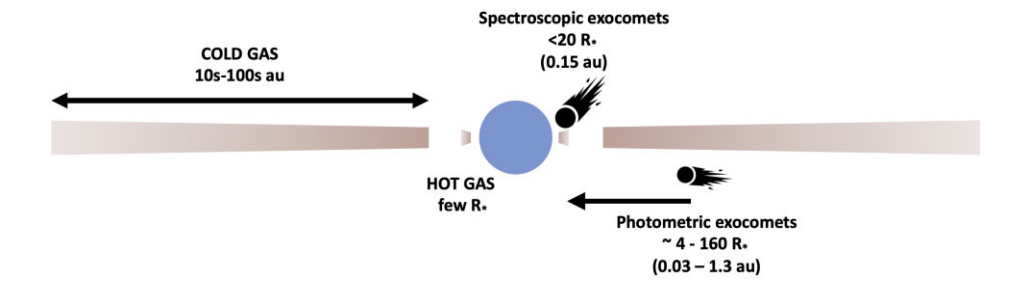


Figure 8. Estimated distribution of gas and exocometary bodies in a typical exocometary system.

greatly any other exocomet host system (Kiefer et al. 2014a). However, the frequency of the photometric exocomets is much lower, with 30 events detected in 156 d through four different TESS sectors (Lecavelier des Etangs et al. 2022). The key to explain this discrepancy could be in the expected stellocentric distances traced by both techniques: While spectroscopic exocomets are expected to be located very close to the star (below $20R_*$, i.e. <0.15 au, Kiefer et al. 2014a; Kennedy 2018), photometric ones are estimated at longer distances (\sim 4–160 R_* , i.e. 0.03–1.3 au with an estimated average distance of 0.18 au; Lecavelier des Etangs et al. 2022). The question remains of whether different exocomet populations could be feeding different gas populations in the disc, i.e. gas detected in emission, much more extended (e.g. Kóspál et al. 2013; Marino et al. 2016; Moór et al. 2017, 2019; Matra et al. 2019; Rebollido et al. 2022) and hot gas detected in absorption, potentially released by exocomets and located closer to the star (e.g. Hobbs et al. 1985; Ferlet et al. 1987; Montgomery & Welsh 2012; Iglesias et al. 2018, 2019; Rebollido et al. 2020). A diagram for the exocomet versus gas location is shown Fig. 8.

However, while the number of exocomets detected in spectroscopy remains larger than those detected in photometry, population D from Kiefer et al. (2014a) is more likely to be in better agreement with the orbital ranges of the photometric populations.

If we translate these exocomet ratios to the observed frequency around 5 Vul in spectroscopy, we would be expecting one photometric transit every 87.36 d, which would be hard to cover with current instrumentation and/or space missions.

5 SUMMARY

Observations performed with *CHEOPS* and *TESS* of the star 5 Vul show no evidence of exocometary activity in the light-curve, despite the exocomet detection in spectroscopy around this star. In this work, we provided an estimation of the sizes and spatial location of the exocomets and a possible explanation for the non-detection of exocometary transits via photometry.

The sporadic nature of exocomets makes it difficult to trace them, as their orbits are almost impossible to constrain. The few efforts to detect the dust counterpart of the exocomets observed in spectroscopy have only been successful for β Pic. This is not surprising, given the high frequency of exocomets, so far much higher than any other. Even for β Pic, only a handful of exocomets have been observed in photometry, contrasting the thousands of events that are reported in spectroscopy. This could potentially be related to the distance at which the exocomets evaporate/sublimate. The estimated distances for Ca II production (where most exocomets have been detected) is just a few stellar radii, much closer to the estimated distances for the photometric observations. This could indicate we are probing two different groups of exocomets: star-grazing comets that sublimate

refractory materials (i.e. calcium), and comets at larger orbits, where the cloud of dust is better sustained.

Lecavelier Des Etangs et al. (1999) estimated dozens of exocometary detections in photometry for large surveys with tens of thousands of stars in the worst-case scenario. However, the results from large missions like *Kepler* and *TESS* show otherwise, with very few detections so far (e.g. Boyajian et al. 2016; Ansdell et al. 2019; Zieba et al. 2019). Given that as of today a large enough sample of stellar ages and spectral types have been observed, the number of detectable exocomets might have been overestimated based on the activity around β Pic.

ACKNOWLEDGEMENTS

We thank the Lorentz Centre for facilitating the workshop 'Exo-Comets: understanding the composition of planetary building blocks' during 2019 May 13-17. The authors are grateful to the staff of the Lorentz Centre and to the scientific organizers of the workshop. CHEOPS is an ESA mission in partnership with Switzerland with important contributions to the payload and the ground segment from Austria, Belgium, France, Germany, Hungary, Italy, Portugal, Spain, Sweden, and the UK. This paper also includes data collected by the TESS mission, obtained from the MAST data archive at the Space Telescope Science Institute (STScI). IR thanks Grant Kennedy for the insightful conversations during the Spirit of Lyot 2022 conference in Leiden. AL and FK acknowledge support from the CNES (Centre National d'études Spatiales, France). This work made use of tpfplotter by J. Lillo-Box (publicly available at: www.github.com/jlillo/tpfplotter), which also made use of the Python packages astropy, lightkurve, matplotlib, and numpy.

DATA AVAILABILITY

Data are available in the CHEOPS and TESS archives: https://cheops-archive.astro.unige.ch/ https://archive.stsci.edu/missions-and-data/tess

REFERENCES

Aller A., Lillo-Box J., Jones D., Miranda L. F., Barceló Forteza S., 2020, A&A, 635, A128

Ansdell M. et al., 2019, MNRAS, 483, 3579

Benz W. et al., 2021, Exp. Astron., 51, 109

Beust H., Morbidelli A., 1996, Icarus, 120, 358

Beust H., Morbidelli A., 2000, Icarus, 143, 170

Boyajian T. S. et al., 2016, MNRAS, 457, 3988

Britt D. T., Consolmagno G. J., Merline W. J., 2006, in Mackwell S., Stansbery E., eds, 37th Annual Lunar and Planetary Science Conference. Lunar and Planetary Science Conference. League City, Texas, p. 2214 Chen C. H., Mittal T., Kuchner M., Forrest W. J., Lisse C. M., Manoj P., Sargent B. A., Watson D. M., 2014, ApJS, 211, 25

Ferlet R., Hobbs L. M., Vidal-Madjar A., 1987, A&A, 185, 267

Fernández Y. R. et al., 1999, Icarus, 140, 205

Gaia Collaboration, 2016, A&A, 595, A1

Gaia Collaboration, 2018, A&A, 616, A1

Grady C. A., Brown A., Welsh B., Roberge A., Kamp I., Rivière Marichalar P., 2018, AJ, 155, 242

Guzik J. A. et al., 2016, ApJ, 831, 17

Hobbs L. M., Vidal-Madjar A., Ferlet R., Albert C. E., Gry C., 1985, ApJ, 293, L29

Hoyer S., Guterman P., Demangeon O., Sousa S. G., Deleuil M., Meunier J. C., Benz W., 2020, A&A, 635, A24

Iglesias D. et al., 2018, MNRAS, 480, 488

Iglesias D. P. et al., 2019, MNRAS, 490, 5218

Jenkins J. M. et al., 2016, in Chiozzi G., Guzman J. C., eds, Proc. SPIE Conf. Ser. Vol. 9913, Software and Cyberinfrastructure for Astronomy IV. SPIE, Bellingham, p. 99133E

Jewitt D., Matthews H., 1999, AJ, 117, 1056

Kennedy G. M., 2018, MNRAS, 479, 1997

Kennedy G. M., Hope G., Hodgkin S. T., Wyatt M. C., 2019, MNRAS, 482, 5587

Kiefer F., Lecavelier des Etangs A., Boissier J., Vidal-Madjar A., Beust H., Lagrange A. M., Hébrard G., Ferlet R., 2014a, Nature, 514, 462

Kiefer F., Lecavelier des Etangs A., Augereau J. C., Vidal-Madjar A., Lagrange A. M., Beust H., 2014b, A&A, 561, L10

Kóspál Á. et al., 2013, ApJ, 776, 77

Kral Q., Matrà L., Wyatt M. C., Kennedy G. M., 2017, MNRAS, 469, 521

Lecavelier Des Etangs A., 1999, A&AS, 140, 15

Lecavelier Des Etangs A., Vidal-Madjar A., Ferlet R., 1999, A&A, 343, 916 Lecavelier des Etangs A. et al., 2022, Sci. Rep., 12, 5855

Lightkurve Collaboration et al., 2018, Astrophysics Source Code Library, record ascl:1812.013 Marino S. et al., 2016, MNRAS, 460, 2933

Marino S., Flock M., Henning T., Kral Q., Matrà L., Wyatt M. C., 2020, MNRAS, 492, 4409

Matra L. et al., 2019, BAAS, 51, 391

Matthews E. et al., 2018, MNRAS, 480, 2757

Montgomery S. L., Welsh B. Y., 2012, PASP, 124, 1042

Moór A. et al., 2017, ApJ, 849, 123

Moór A. et al., 2019, ApJ, 884, 108

Morales F. Y. et al., 2009, ApJ, 699, 1067

Musso Barcucci A. et al., 2021, A&A, 645, A88

Pavlenko Y., Kulyk I., Shubina O., Vasylenko M., Dobrycheva D., Korsun P., 2022, A&A, 660, A49

Pecaut M. J., Mamajek E. E., 2013, ApJS, 208, 9

Rappaport S. et al., 2018, MNRAS, 474, 1453

Rebollido I. et al., 2020, A&A, 639, A11

Rebollido I. et al., 2022, MNRAS, 509, 693

Redfield S., Linsky J. L., 2008, ApJ, 673, 283

Ricker G. R. et al., 2015, J. Astron. Telesc. Instrum. Syst., 1, 014003

Roberge A., Feldman P. D., Lagrange A. M., Vidal-Madjar A., Ferlet R., Jolly A., Lemaire J. L., Rostas F., 2000, ApJ, 538, 904

Smith J. C. et al., 2012, PASP, 124, 1000

Strøm P. A. et al., 2020, PASP, 132, 101001

Stumpe M. C. et al., 2012, PASP, 124, 985

Stumpe M. C., Smith J. C., Catanzarite J. H., Van Cleve J. E., Jenkins J. M., Twicken J. D., Girouard F. R., 2014, PASP, 126, 100

Vidal-Madjar A. et al., 1994, A&A, 290, 245

Yoon J., Peterson D. M., Kurucz R. L., Zagarello R. J., 2010, ApJ, 708, 71
 Zieba S., Zwintz K., Kenworthy M. A., Kennedy G. M., 2019, A&A, 625, L13

This paper has been typeset from a T_EX/IAT_EX file prepared by the author.